Polym. Bull. (2012) 69:1053–1071
DOI 10.1007/s00289-012-0779-x

ORIGINAL PAPER

Determination of crystallization parameters and occurrence of *trans*-reaction in a ternary polymer blend system

Adam Al-Mulla

Received: 14 December 2011 / Revised: 10 March 2012 / Accepted: 22 May 2012 /

Abstract Differential scanning calorimetry (DSC) results under non-isothermal cooling conditions of a blend consisting of polytrimethylene terephthalate (PTT)/polybutylene terephthalate (PBT)/and polycarbonate (PC) in the ratio 25:25:50 wt% are reported. Kissinger and Matusita models were used to evaluate the kinetic parameters for the crystallization process for the neat polyesters and the blend. Probable growth mechanisms which occur during the transformation from amorphous to crystalline state are discussed. The blend system comprising of semicrystallizable polyesters and an amorphous polycarbonate was characterized for possible *trans*-reaction occurring in the system using differential scanning calorimeter, proton nuclear magnetic resonance (^{1}H NMR), and Fourier transform infrared spectroscopy (FT-IR) analysis. DSC analysis of the blend indicated that it is an immiscible system. ^{1}H NMR and FT-IR analysis indicate that no chemical *trans*-reaction is found to have occurred between these three polymers. Based on these results it can be justified that transesterification was not a necessary condition for miscibility in PTT/PBT/PC blend.

Keywords Ternary blend · Crystallization kinetics · Transesterification reaction

Introduction

Polymeric blends are a rapidly growing field in material science and engineering and have attracted a lot of attention in the academic and industrial communities. Blending of aromatic engineering polymers has excellent properties even when the blends are immiscible [1, 2]. Good adhesion due to interaction among the aromatic rings of these polymers may be one of the reasons for the observed behavior [2].

A. Al-Mulla (✉)
Department of Chemical Engineering, Kuwait University, P.O. Box 5969, 13060 Safat, Kuwait
e-mail: a.almulla1@ku.edu.kw

A newly developed polyester, PTT has structure and properties intermediate between those of PET and PBT [3, 4]. Some of the poor performance properties of PTT like low heat distortion temperature, low melt viscosity, poor optical properties, and pronounced brittleness at low temperature have restricted its use as a desirable engineering plastic. Some of the former properties can be improved by developing blends of PTT with PBT and PC [5–8].

The polyesters (PET/PTT/PBT) can possibly undergo *trans*-reactions with PC at high temperatures in the solid state and in the melt, like alcoholysis or direct ester interchange, which can affect its miscibility and in some cases induce worsening of material properties. The phase structure [9–12], and crystalline behavior [10, 12–18] of PTT/PC blends have been reported. The blends were shown to be partially miscible [9–12] with different miscibility levels. Plausible exchange reactions could give rise to the homogenization of the blends and eventually lead to single-phase material. The presence of PC could hinder PTT and PBT crystallization in the blend [13] decreasing the level of crystallinity [16–18] by means of interchange reactions.

Non-isothermal heating and cooling techniques using different thermal analysis machines like DSC and TGA are being used in studying various reactions. (Example: surface reactions, diffusion controlled reactions, and other physical-decomposition reactions such as phase transformation and nucleation [19–24].) Various solid-states kinetic mechanisms have been discussed in the literature, most of which have been applied to relatively simple systems. These reaction mechanisms could be useful in explaining the route of solid-state reactions. The concentration term in solid-state reactions is less clearly defined; therefore the extent of conversion, α, is predominantly used. The quantity α is sometimes called the fractional conversion or fraction converted. Many different reaction mechanisms have been proposed to describe solid-state reactions, some of which have been used in this paper. These reaction mechanisms can be expressed in a differential form, $f(\alpha)$ as well as an integral form, $g(\alpha)$.

In this study, the crystallization kinetics of the blend (PTT/PBT/PC) and neat polyesters (PTT and PBT) were investigated as a function of crystallization temperature. The addition of a third component (amorphous PC) could affect the properties of the crystalline phase of the crystallizable component including the overall crystallinity. Hence, an understanding of the crystallization kinetics of this semi crystalline polymer blend is essential for controlling the processing conditions and consequently the utility of the material for a given application.

Another objective of this study was also to check if an exchange reaction takes place when a physical mixture is formed or if *trans*-reactions occur during melt blending temperatures and time, and if *trans*-reactions are necessary to from a single phase.

Experimental

Materials

PTT and PBT with number average molecular weight ($\overline{M_n} = 28{,}000$ and 26,000 (g/mol)) used here was a product of Century Enka. Ltd. (India). PC obtained from

Bisphenol A was also purchased from the same company and had a $\overline{M_n}$ of 30,000 (g/mol).

Blend preparation

PTT/PBT/PC (25:25:50 wt%) pellets were dried for 6 h at 120 °C in an oven. These were mixed by vigorous shaking and mechanically blended in single-screw extruder at a screw speed of 50 rpm and extruder barrel temperature zones of 275, 280, and 268 °C. The strands from the extruder was cooled in a water bath and pelletized. The pellets were later dried at 110 °C for 6 h. A second pass was carried out under the same extrusion conditions using these pellets. These strands were cooled, pelletized, and dried under identical conditions and stored in a desiccator.

^{1}H NMR (nuclear magnetic resonance) analysis

The ^{1}H NMR spectra of the neat polymers and the blend was obtained by dissolving the polymers in deuterated chloroform/deuterated trifluroacetic acid ($CDCl_3$/CF_3COOD) (85/15, wt/wt) using Bruker AMX 300 instrument. The co-polyester content was determined from signal intensities of the terephthalate centered triads in the ^{1}H NMR spectrum.

FT-IR analysis

The samples were dried in vacuum at 110 °C for 12 h to remove any moisture before analysis was carried out. The samples were analyzed by FT-IR spectroscopy (Bruker KFS-66). The analysis was carried out on microtome cuts of thickness 2–3 μm. The lateral resolution was 20 and 200 μm, respectively.

The spectral resolution was 2 cm^{-1} and the scans were repeated till consistency was obtained.

Non-isothermal differential scanning calorimetric (DSC) analysis

A Perkin-Elmer diamond DSC 7 apparatus was used for measuring the non-isothermal crystallization kinetics in the cooling mode from the molten state (melt crystallization). The thermal response of the instrument was calibrated from the enthalpy of fusion of a known mass of indium (99.99 % pure). The temperature scale of the calorimeter was calibrated using the melting points of indium and lead. Plots of actual against experimental melting points were linear and used to calibrate the calorimeter temperature directly after correction for thermal lag by extrapolation to zero heating rate. All measurements were carried out in a nitrogen (N_2) atmosphere. To determine the glass transition temperature of PTT, PBT, PC and their blend, each sample (4–5 mg) encapsulated in an aluminum pan, was first heated in the DSC cell from 30 °C at a heating rate of 80 °C/min to 280 °C where it was kept for 5 min in order to remove previous thermo-mechanical history. Then, it was taken out from the DSC cell and immediately submerged in N_2(l) to attain the

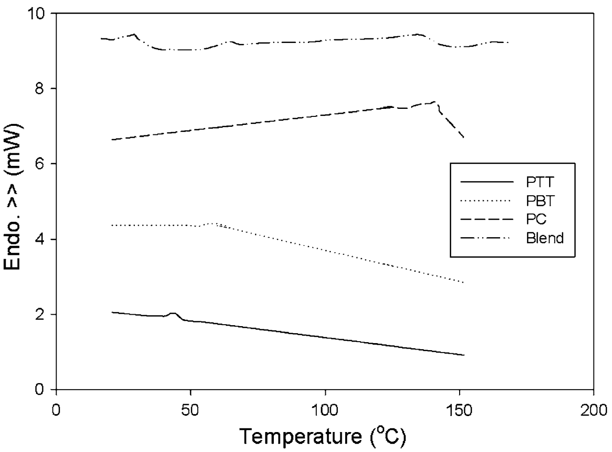

Fig. 1 DSC thermograms of PTT, PBT, PC, and blend at 10 °C/min

completely amorphous state of the sample. After 10 min of submersion in N_2(l), the sample was transferred back to the DSC cell where it was reheated from 25 °C at a heating rate of 10 °C/min to 280 °C. This treatment allows the determination of glass transition temperature (T_g). For non-isothermal melt crystallization, all the samples (4–5 mg) were heated to 280 °C and kept for 5 min in the DSC cell and rapidly cooled to the crystallization temperature (T_c) to remove the thermal history. Then the samples were cooled at constant rates of 5, 10, 15, and 20 °C min^{-1}, respectively. The exothermic curves of heat flow as a function of time were recorded and investigated.

Results and discussions

Figure 1 shows the DSC melting thermograms for N_2(l) quenched PTT, PBT, PC and blend recorded during heating with a heating rate of 10 °C/min. The glass transition temperature of PTT, PBT, and PC were found to be 45, 66, and 149 °C, respectively. These values are found to be in agreement with the literature values reported for these polymers.

DSC thermograms were recorded for the neat polymers (PTT and PBT) at different cooling rates of 5, 10, 15, and 20 °C/min. The exothermic peaks at different cooling rates (β) for different polyesters and the blend are shown in Fig. 2. As evident from this figure, the peak temperature, T_p, decreases with increasing cooling rates (β) for the blend. With increasing cooling rate, the exothermic trace shifted toward lower temperatures (Fig. 2) [25, 26]. The observations are general for both pure and blend samples. The single crystallization exotherm for the blend for each cooling rate suggests that all the components crystallized at the same time. The values obtained for the blend, at all the cooling rates were found to be lower than that of neat PTT, while those obtained for higher cooling rates were found to be higher than those of pure PTT (Table 1). These results possibly suggest that the presence of less crystallizable (possibly PTT and PC) molecules in the blend reduced the crystallisability of the blend and the mechanism for non-isothermal melt crystallization depended very much on the cooling rate used.

The crystallization process is usually considered to consist of two stages, a primary and a secondary stage. The primary crystallization consists of a fast outward growth of the lamellar stacks until impingement. The secondary crystallization, which sometimes overlaps the primary crystallization, involves the filling of the spherulites interstices and proceeds at a much slower rate than the primary crystallization [8]. The relative degree of crystallinity, $\alpha(t)$, at time, t, can be described as the area obtained from the DSC exothermic peak at time, t, divided by the total final area under the exothermic peak as shown in the below equation.

$$\alpha(t) = \frac{\int_{T_i}^{T_C} \left(\frac{dH}{dT}\right) dT}{\int_{T_i}^{T\infty} \left(\frac{dH}{dT}\right) dT} \quad (1)$$

T_c is the arbitrary crystallization temperature at time, t, T_i is the arbitrary initial crystallization temperature, and T_∞ is the arbitrary temperature at which the crystallization process is completed. Therefore, the relative crystallinities of PTT/PBT/PC (25:25:50 wt%) blend at a crystallization time, t, or a crystallization temperature, T, can be obtained by dealing with the DSC curves using Eq. (1). Figures 3 and 4 illustrate the variations of relative crystallinities of the blend with the crystallization time and the crystallization temperature. The time to reach a given relative crystallinity decreased as the heating rate increased. The temperature span for the onset of crystallization ($T_{0.01}$) at different heating rates for PTT varied from 155 to 180 °C and the end point of crystallization ($T_{0.99}$) varied between 185 and 196 °C. For PBT, $T_{0.01}$, varied between 164 and 187 °C and, $T_{0.99}$ varied between 201 and 208 °C. The blend showed, $T_{0.01}$, between 161 and 184 °C and, $T_{0.99}$, between 192 and 200 °C (Table 1). As seen in Table 1 the values for the onset and endset are found to decrease with increasing cooling rates.

The peak crystallization temperatures obtained from the cooling scans as a function of cooling rate are plotted in Fig. 5. Single-crystallization exotherm was observed during cooling, and the position and magnitude of the exotherm are dependent on the cooling rate. The peak cooling temperature for the blend is found to lie intermediate between that of PTT and PBT. The values of T_p are found to decrease with increasing cooling rates (Table 1).

Crystallization kinetics

Crystallization kinetic studies can help to determine the nucleation and crystal growth mechanism of the phases formed. Different equations are used to evaluate the activation energy for the crystallization of polymeric blends. One of the important equation used in this paper to determine non-isothermal DSC data, is the Kissinger equation [22], which is based on the analysis of the variation of the maximum peak temperature with the heating rate.

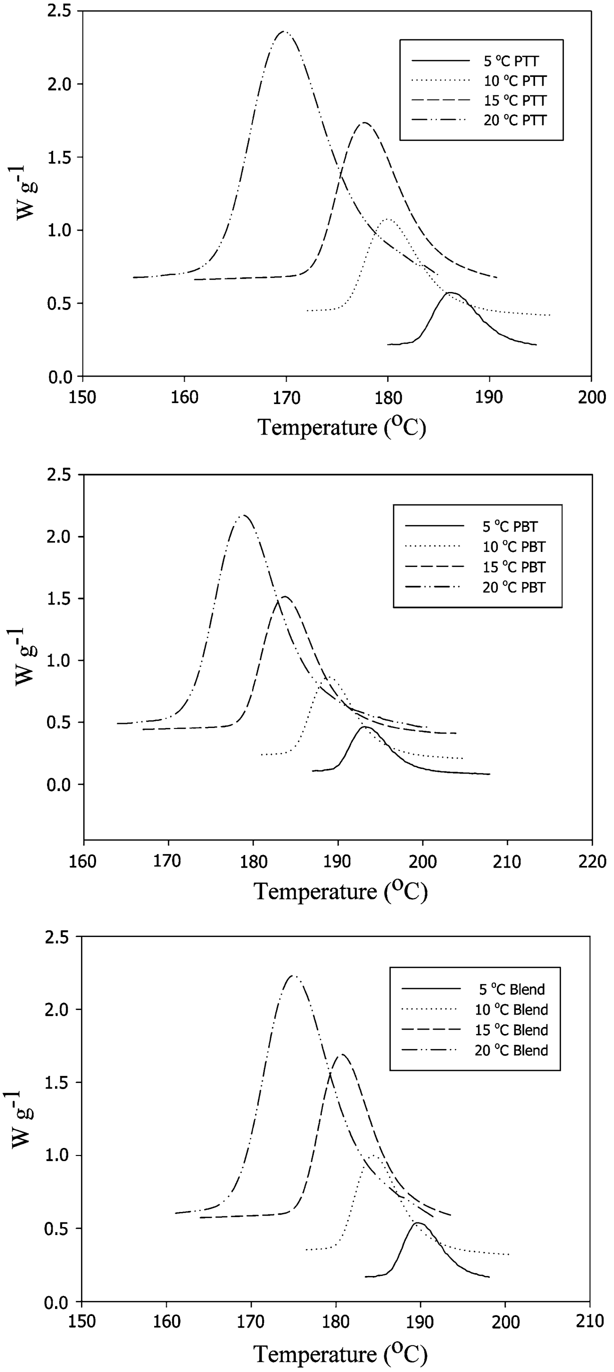

Fig. 2 The exothermic peak traces at different cooling rates

Table 1 Parameters of non-isothermal crystallization kinetics of neat polymers and blend

	Cooling rates (°C/min)	H_c (J mol^{-1})	Kissinger equation		Matusita equation		$T_{0.01}$ (°C)	$T_{0.99}$ (°C)	T_p (°C)	χ
			E (kJ mol^{-1})	LnA	E (kJ mol^{-1})	LnA				
PTT	5	−47.4	155	51	159	59	180	196	187	0.509
	10	−41.7					172	195	179	0.513
	15	−42.6					161	191	175	0.521
	20	−51.6					155	185	171	0.515
PBT	5	−40.6	185	58	184	74	187	208	194	0.520
	10	−43.5					181	205	188	0.518
	15	−44.8					167	204	184	0.523
	20	−56.2					164	201	180	0.515
Blend	5	−45	183	58	180	67	184	200	191	0.512
	10	−42.6					177	198	184	0.523
	15	−42.8					164	194	181	0.531
	20	−52.3					161	192	177	0.508

H_c enthalpy of crystallization (J mol^{-1}), χ crystalline fraction

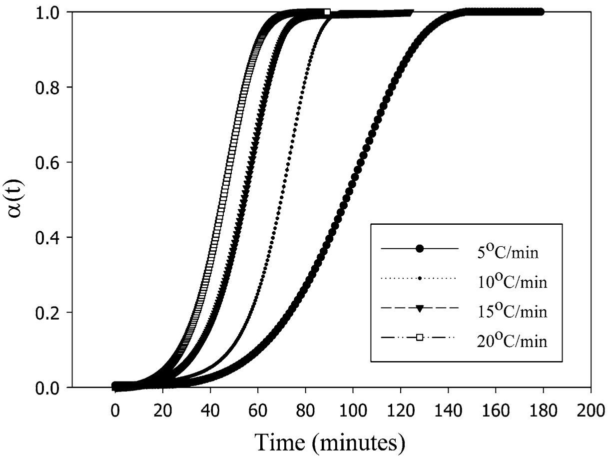

Fig. 3 Variations of relative crystallinities of PTT/PBT/PC blend with crystallization time

The Kissinger equation is the only equation that refers to the crystallization process by considering the surface/bulk nucleation mechanism and the dimensionality of crystal growth. The expression given by Matusita and co-workers [23, 24] for the modified Kissinger equation for a non-isothermal measurement is

$$\ln\left(\beta^n/T_p^2\right) = -mE_c/RT_p + \text{constant} \tag{2}$$

where E_c is the activation energy for crystallization (J mol^{-1}); R is the gas constant (8.314 J mol^{-1} K^{-1}), T_p is the maximum temperature of the exothermic

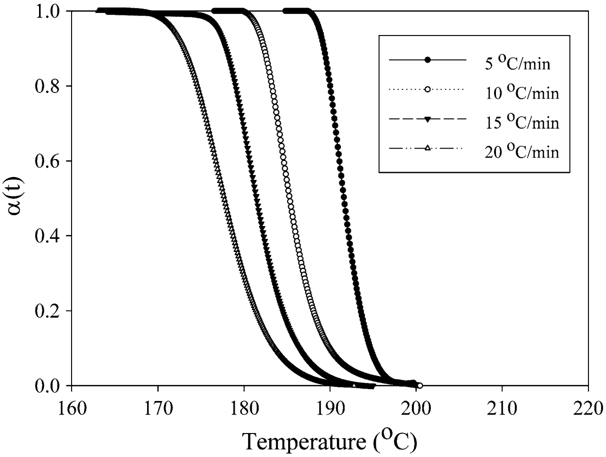

Fig. 4 Variation of relative crystallinities of the blend with crystallization temperature

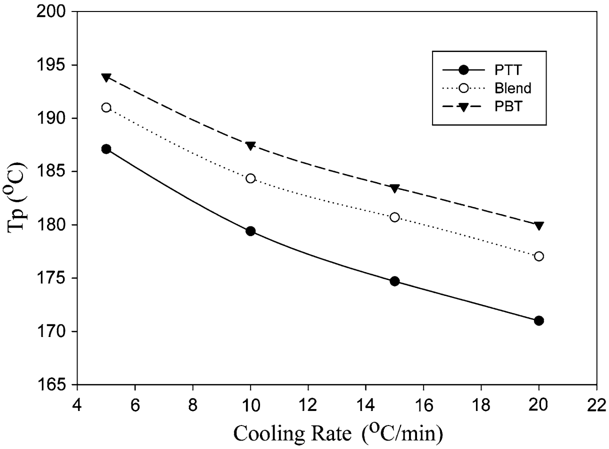

Fig. 5 Variation of peak temperature of crystallization as a function of cooling rate for the neat polymers and blend

crystallization peak (K), n is order of crystallization and a constant known as the Avrami parameter, m represents the dimensionality of crystal growth, and β is the heating rate (°C min^{-1}). Dividing mE_c by m, the activation energy for crystal growth can be obtained. Only when the surface nucleation is dominant, in other words, $n = m = 1$ for all the heating rates, Eq. (2) is identical with the so-called Kissinger equation [23–26]:

$$\ln\left(\beta/T_p^2\right) = -E/RT_p + \text{constant} \tag{3}$$

where E is the Kissinger activation energy for crystallization.

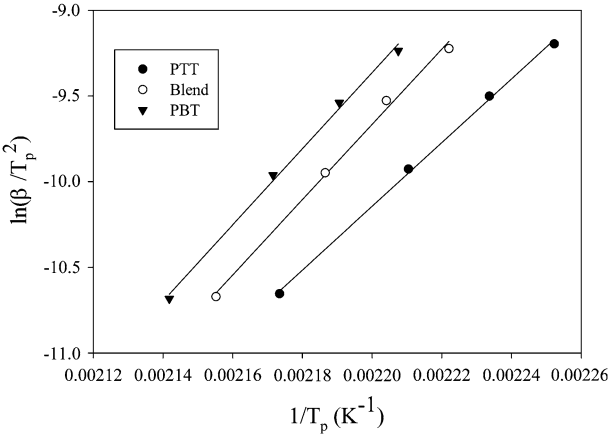

Fig. 6 $\ln(\beta/T_p^2)$ versus $1/T_p$ plot for blend with a linear fit (−)

According to Kissinger's formula [27], the peak temperature for crystallization (T_p) depends on the heating rate (β) as indicated in Eq. (3). The kinetic parameters have been calculated for the modified Kissinger model using Eq. (3). Plotting ln (β/T_p^2) versus $1/T_p$ should give straight lines. The straight lines shown in Fig. 6 give a linear fit with the experimental results of the blend.

The slope of each line gives the activation energy (E) for crystallization. The values of E for the neat polymers and the blend were calculated and listed in Table 1. The results obtained indicate that the value of E for the blend is in between that of PTT and PBT. This possibly suggests that PTT crystallizes faster than the blend indicating that the effective energy barrier governing the non-isothermal crystallization of the blend is higher than PTT.

Another approach tried for obtaining the crystallization parameter for the kinetics of crystallization is by using the method specifically suggested for non-isothermal conditions by Matusita et al. [28]. The crystallization mechanism of amorphous materials is controlled by nucleation and growth process, which can be characterized by the activation energy and dimensionality of the growth process. According to Matusita, for the fraction crystallized, χ, the non-isothermal crystallization is given by:

$$\ln[-\ln(1-\chi)] = -n\ln\beta - 1.052\,mE/RT + \ln A, \tag{4}$$

where n, 1.052 and m are constants that depend on the nucleation and growth mechanism, E is the activation energy of crystallization, and A (s^{-1}) is the pre-exponential factor. Crystallized volume fractions, χ, are shown in Table 1 and are determined from DSC curves. The values for the neat polymers and the blend are indicated in Table 1. The volume fraction crystallized, χ, at any temperature T, is given by$\chi = (S_T/S)$ where S_T is the area between any two temperature intervals. S is the area of the exothermic peak between the temperature T_o, where the crystallization just begins and any temperature on the crystallization curve.

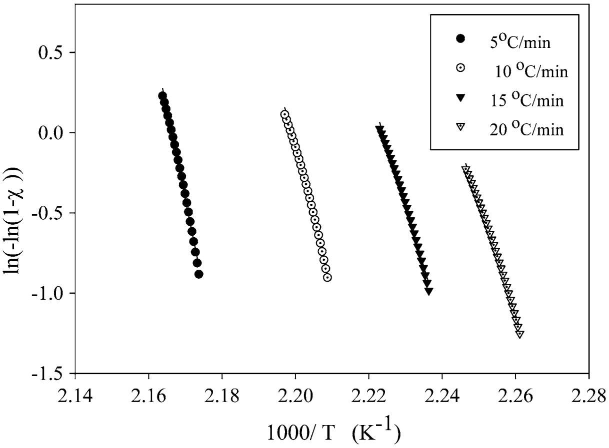

Fig. 7 Plot of ln(−ln(1−χ)) versus 1/T for PTT at different heating rates

For a quenched polymer containing no nuclei $n = m + 1$ and for a polymer which have sufficiently large nuclei before carrying out DSC experiment, is $n = m^9$. Considering the fact that this analysis is based on polyesters having large number of nuclei, the constant m is taken to be $m = n$. For obtaining the crystallization kinetic parameters, $n = 1$ was considered for the modified Kissinger equation, and the same value was considered for n in the Matusita equation.

The plot of $\ln[-\ln(1 - \chi)]$ versus $1/T$ for PTT measured at different heating rates, showed slight deviation from linearity for all the heating rates as seen in Fig. 7. Similar deviations were reported for other crystallizable materials [29] and were attributed to the saturation of nucleation sites in the final stages of crystallization [30]. In this analysis, the activation energy is calculated from the slopes of the linear fits ($r > 0.99$) to the experimental data from a plot of $\ln-\ln(1 - \chi)]$ versus $1/T$. The E values calculated from the slope for each of the polymers are reported in Table 1. Even though the curves show some deviation from the linear fit, employing one value for E was sufficient to fit the experimental values. The E values seem to be independent of the heating rate, and therefore, an average value was obtained for all the heating rates.

Determination of kinetic mechanism

For the determination of the most probable mechanism function the theoretical basis of the non-isothermal kinetic theory of thermal decomposition of solid materials is considered [19]. Gao et al. [31] have plotted $\ln g(\alpha)$ versus $\ln(\beta)$ using linear regression least square method. In this study, it was stated that if the mechanism under consideration confirms to a certain $g(\alpha)$, the slope k should be equal to -1.000 and correlation coefficient r should be equal to 1 [32].

In this study, an appropriate temperature was selected (190 °C) such that the conversion value (α) at this temperature for different cooling rates could be

Table 2 Kinetic parameters obtained from $\ln g(\alpha)$ versus $\ln(\beta)$ curves for 30 types of mechanism functions at $T = 190$ K and $\beta = 5, 10, 15$, and 20 °C/min for PTT, PBT, and blend

Function no.	Integral form $g(\alpha)$	PTT			PBT			Blend		
		B	*k*	*r*	*B*	*k*	*r*	*B*	*k*	*r*
1	α + (1−α)*ln(1−α)	7.896	−3.600	0.927	9.971	−5.801	0.937	11.460	−7.402	0.987
2	(1−(1−α)^1/3)^2	2.833	−0.983	0.889	1.428	−0.894	0.981	−0.132	−0.313	0.711
3	(1−2*α/3)−(1−α)^2/3	−2.002	0.588	0.965	−1.987	0.601	0.913	−0.802	0.152	0.640
4	(−ln(1−α))	12.313	−5.106	0.963	8.602	−4.072	0.995	2.014	−1.878	0.976
5	(−ln(1−α))^2/3	16.881	−9.431	0.889	16.106	−8.143	0.995	2.930	−3.757	0.976
6	(−ln(1−α))^1/2	8.638	−4.020	0.965	7.909	−4.071	0.995	6.412	−4.071	0.994
7	(−ln1−α))^1/3	8.909	−4.020	0.965	7.504	−4.072	0.995	6.006	−4.071	0.994
8	(−ln(1−α))^1/4	9.503	−4.020	0.965	7.216	−4.072	0.982	5.719	−4.071	0.994
9	1−(1−α)^1/4	0.3369	−3.072	0.978	0.337	−0.212	0.981	0.337	−0.174	0.981
10	1−(1−α)^1/3	0.637	−0.301	0.989	0.476	−0.298	0.981	0.290	−0.248	0.868
11	1−(1−α)^1/2	0.988	−0.637	0.965	0.818	−0.508	0.980	0.524	−0.432	0.878
12	α	3.567	−1.464	0.912	4.609	−2.647	0.912	5.663	−3.552	0.994
13	α^3/2	11.213	−5.082	0.965	13.13	−7.940	0.912	16.296	−10.657	0.982
14	α^1/2	3.915	−2.647	0.855	3.915	−2.647	0.912	3.915	−2.647	0.912
15	α^1/3	2.167	−1.364	0.966	3.509	−2.646	0.912	4.564	−3.552	0.982
16	α^1/4	2.912	−1.366	0.989	3.915	−2.647	0.912	4.277	−3.552	0.982
17	((1−α)^−1/2)−1	15.392	−7.125	0.977	12.356	−5.678	0.993	7.298	−4.391	0.996
18	((1−α)^−1)−1	16.034	−8.129	0.962	15.992	−6.219	0.892	5.516	−2.650	0.977
19	(1−α)^2	30.143	−14.011	0.952	28.235	−10.160	0.833	6.645	−2.396	0.819
20	(1−(1−α)^2)	0.312	−0.101	0.974	1.659	−0.927	0.849	5.304	−3.175	0.963
21	(1−(1−α)^3)	2.263	−0.379	0.965	3.331	−1.834	0.808	4.941	−2.901	0.942
22	(1−(1−α)^4)	1.775	−0.629	0.823	2.975	−1.622	0.780	4.646	−2.695	0.921

Table 2 continued

Function no.	Integral form $g(\alpha)$	PTT			PBT			Blend		
		B	*k*	*r*	*B*	*k*	*r*	*B*	*k*	*r*
23	(−ln(1−α))^2	19.871	−8.143	0.923	17.204	−8.143	0.995	14.210	−8.143	0.994
24	(−ln(1−α))^3	17.763	−12.215	0.997	25.806	−12.215	0.995	21.314	−12.214	0.994
25	(−ln(1−α))^4	36.2	−16.278	0.966	34.400	−16.286	0.995	28.419	−16.286	0.995
26	(1−(1−α)^0.5)^0.5	2.596	−1.389	0.993	2.649	−1.568	0.957	2.739	−1.940	0.994
27	(1−(1−α)^(1/3))^0.5	3.766	−1.598	0.998	2.788	−1.690	0.972	1.776	−1.018	0.990
28	(−ln(1−α))^(1/4)	3.823	−1.009	0.996	2.151	−1.018	0.995	1.776	−1.010	0.995
29	(1/3)*α^(1/3)	0.234	−0.990	0.963	0.438	−0.882	0.912	0.789	−1.184	0.982
30	(1/2)*α^(1/2)	1.806	−1.465	0.963	1.611	−1.323	0.912	2.138	−1.776	0.982

B intercept, *k* slope, *r* correlation coefficient

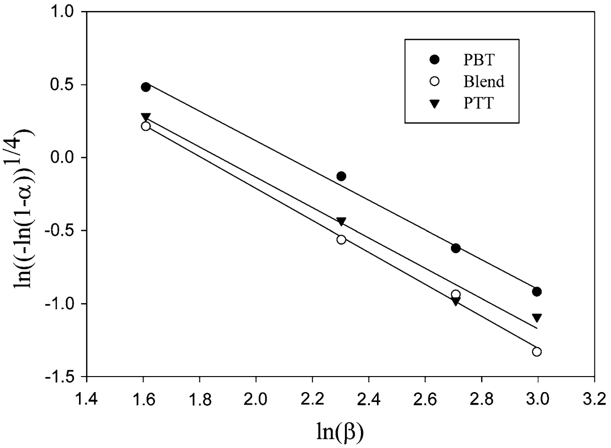

Fig. 8 Plot of ln[(−ln(1−α)$^{1/4}$] versus ln(β) depicting the most probable mechanism for PTT, PBT, and blend at 190 °C

obtained. The crystallization temperature ranges for different conversions for 5, 10, 15, and 20 °C/min at 190 °C is illustrated in Table 1. To determine the appropriate equation governing the crystallization process, the conversion value at $T = 190$ °C was put into different types of reaction mechanism functions for PTT, PBT, and blend crystallization data. Table 2 summarizes the integral form, $g(\alpha)$ functions for 30 different types of kinetic mechanisms used for describing solid-state reactions. The slope (k), correlation coefficient (r), and intercept B of the linear regression of ln$g(\alpha)$ versus ln(β) (β = cooling rate) were obtained. The parameters in Table 2 indicate that the slope of function number 28 are almost close to −1 and has a correlation coefficient (r) greater than 0.98 compared to others. Figure 8 depicts a plot of ln[(−ln(1−α)$^{1/4}$] versus ln(β) for PTT, PBT, and blend at 190 °C. This plot shows that the crystallization data obtained can be modeled using AE2 mechanism (function number 28, Table 2). The kinetic analysis of the isothermal runs at 190 °C revealed agreement with AE2 mechanism which involves random nucleation followed by the growth of nuclei of a defined dimensionality. The Avrami–Erofeev (AE2) equation is given as [33]:

$$[-\ln(1-\alpha)]^{1/n} = g(\alpha) \tag{5}$$

Here, n takes the value 4. Avrami–Erofeev models have been observed for typical crystallization kinetics. Obedience to the AE2 equation is often considered sufficient proof to identify the mechanism of a liquid to solid-state transformation [19] as a nucleation and growth kind. This growth could occur in the presence or absence of nuclei.

It is known that transesterification in polyester blends can affect the crystallization behavior of PTT and PBT in the blend [34, 35]. The *trans*-reaction between PTT, PBT, and PC in the blend was analyzed by ^{1}H NMR spectroscopy. Figure 9 shows the spectra of the blend and neat polymers. The spectra of the blend shows all

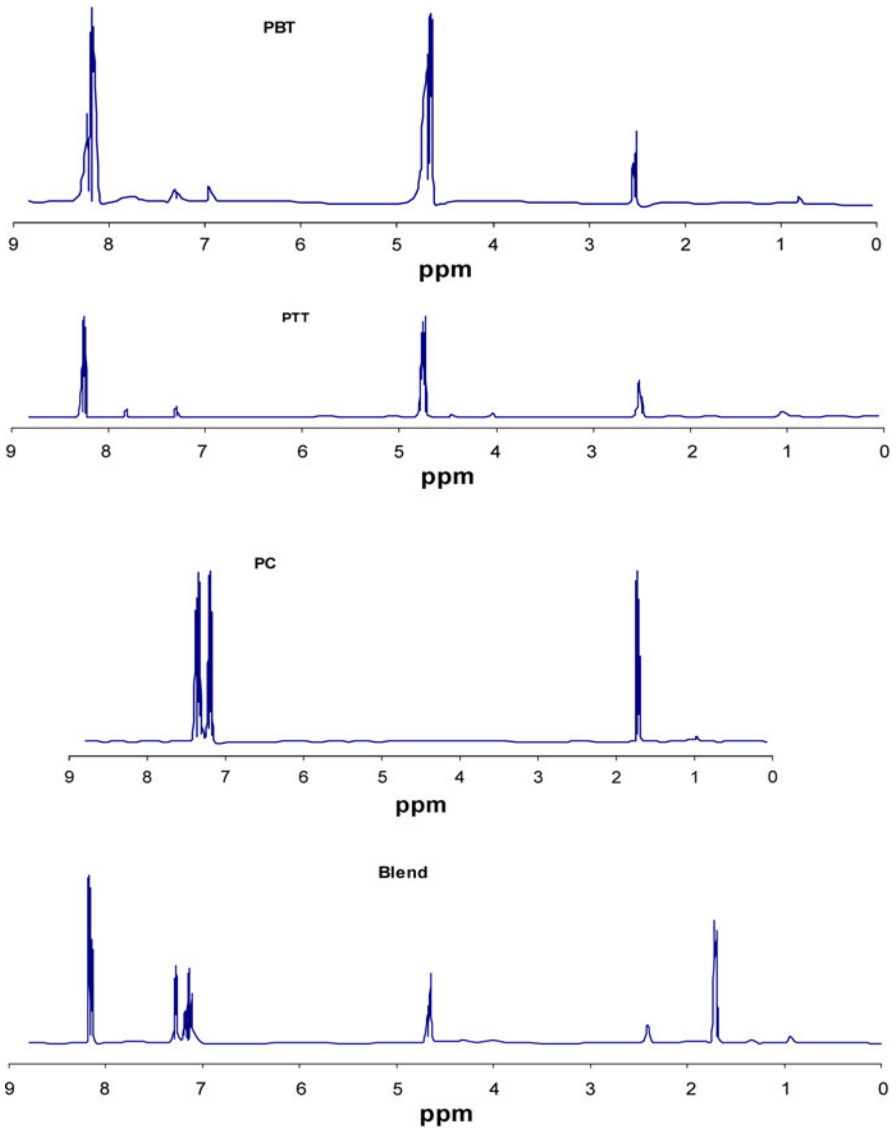

Fig. 9 ^{1}H NMR spectra for neat polymers and the blend

the characteristic peaks of neat PTT, PBT, and PC with no new peaks, indicating that no detectable chemical changes occurred in the blend due to *trans*-reaction.

To check that *trans*-reaction did not affect the crystallization data, DSC studies were carried on the blend. The sample was heated at a rate of 20 °C/min from room temperature to 265 °C, held at 265 °C for 5 min to remove any thermal history, and subsequently cooled to room temperature at a rate of 10 °C/min. The sample was then reheated from 30 to 265 °C at a rate 10 °C/min to observe its melting behavior.

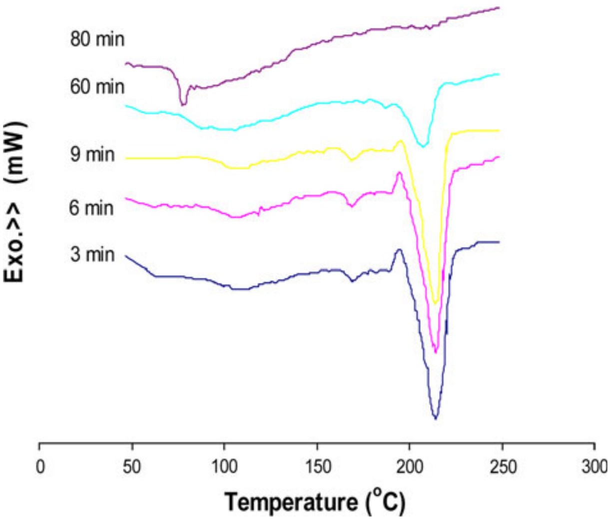

Fig. 10 DSC heating scan of the blend sample melt annealed at 265 °C for various time and subsequently cooled to room temperature

This cycle was applied thrice to the same sample for different time periods (Fig. 10) until transesterification was observed. It was found from the DSC heating curves that melt annealing of the blend at 265 °C for 3, 6, and 9 min did not produce any significant changes in the melting endothermic peak of the blend. In contrast, sample melt annealed at 265 °C for 60 min shows a depression in the melting point as well as a reduction in the melting enthalpy of the blend. Eventually, at extended annealing times (80 min) the melting endothermic peak of the blend disappeared. This effect can plausibly be attributed to some *trans*-exchange reaction between PTT, PBT, and PC components during the extended annealing period. These experiments confirm the assumption that the crystallization data of a blend sample, held at 265 °C for a period of time shorter than 9 min is not influenced by transesterification reaction.

Chemical reactions could occur between PTT, PBT, and PC chain segments of the blend upon annealing at high temperatures. The blend was heated to 265 °C and held constant for 9 and 80 min to induce *trans*-reaction of various extents. The heated blends then possibly contained PTT, PBT, and PC and certain fractions of an exchanged random copolymer of PTT–PBT–PC segments. The transesterified product will readily dissolve in dichloromethane and should contain mostly the amorphous random copolymer (product of the *trans*-reactions) and unreacted PC homopolymer (which is soluble in dichloromethane), while the insoluble portion will contain mainly the un-exchanged PTT, PBT homopolymer that is insoluble in dichloromethane. For FT-IR analysis, the heated blends were extracted in dichloromethane-solvent into soluble and insoluble portions. The extracted soluble portion and insoluble portion were characterized with FT-IR analysis. Figure 11 shows the C=O stretching bands for the soluble portion and insoluble portion of the blends heated at 265 °C for different times; (A) 9 min, and (B) 80 min. The C=O

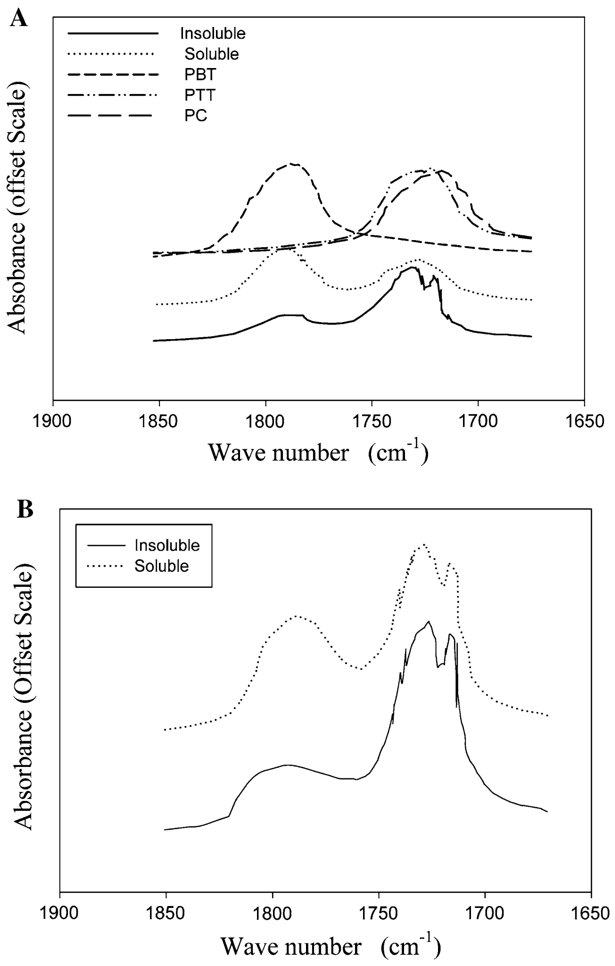

Fig. 11 FT-IR spectra showing C=O stretching bands for the soluble portion versus insoluble portion of the neat polymers and blend heated at (265 °C) for different times. **a** 9 min. **b** 80 min

stretching bands of the carbonyl group in neat PC, PTT, and PBT were observed at 1780, 1720, and 1710 cm^{-1}, respectively. The absorption peaks at 1,720 and 1,710 cm^{-1} characteristic of the C=O stretching of PTT and PBT chain segment, was found in the spectra of the soluble portion and its intensity increased with the annealing time imposed on the samples. In addition, the absorption peak of the PC, C=O stretching at 1,780 cm^{-1} was revealed with less intensity in the IR spectra of the insoluble portion and the intensity also increased with annealing time. The 1,720 and 1710 cm^{-1} peak (in the soluble portion spectra obtained for long-reaction period of 80 min) might be attributed to the C=O stretching of PTT and PBT chain fragment linked on the reaction-occurred copolymer backbone in the soluble portion, and the 1,780 cm^{-1} absorption peak (in the insoluble portion spectra) was believed to be associated with the C=O stretching of the PC segments in the

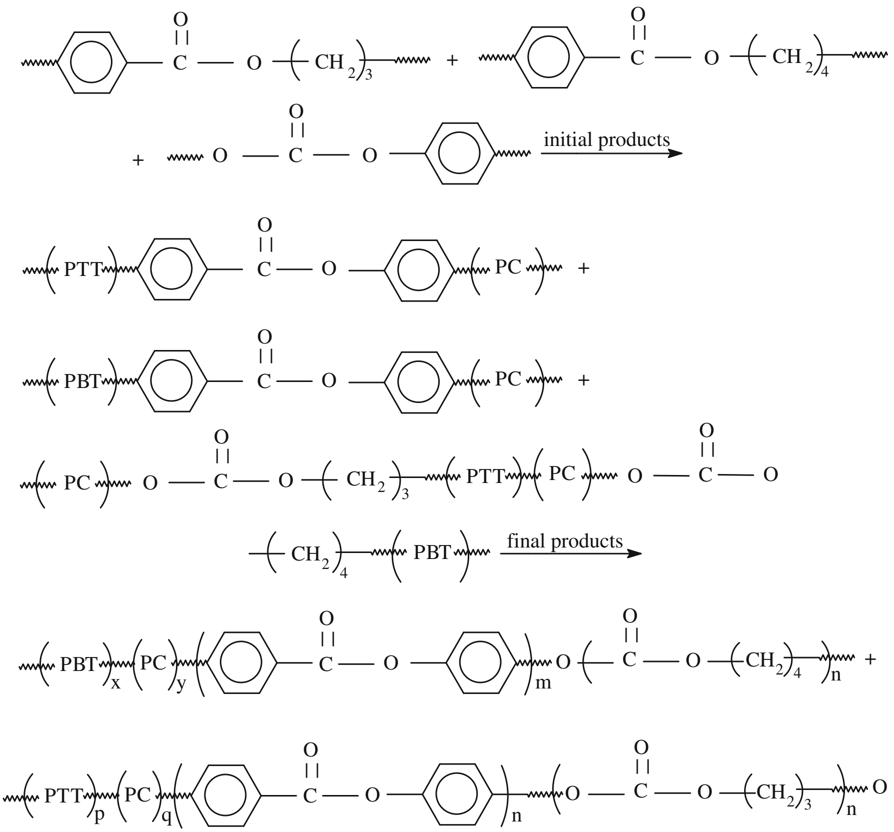

Scheme 1 Transesterification in PTT/PBT/PC blend

copolymer in the insoluble portion. In other words chemical reaction occurred upon annealing at high temperature for long-time period (>9 min) and chain segments of PTT, PBT, and PC exchanged with each other, especially between the ester structures of two homopolymers.

From, observation and analysis of the FT-IR spectra, a possible mechanism about transesterifications between PTT, PBT, and PC for long-time periods at 265 °C can be proposed as shown in Scheme 1.

This mechanism shows that the carbonyl groups of PTT and PBT are exchanged with the carbonate groups in PC upon annealing for long times at high temperatures, and the exchange leads to formation of possibly a new product that is comprised of the exchanged PTT/PBT/PC segments.

Conclusions

Analysis of the non-isothermal crystallization data indicated that both Kissinger and Matusita models are reliable methods for the estimation of crystallization kinetic parameters for neat PTT, PBT, and blend. The values of activation energies using both these models are quite close. Based on the analysis of crystallization kinetic data, using thirty different reaction mechanisms, function number 28 with $g(\alpha) = -\ln(1-\alpha)^{1/4}$ was found to be the most appropriate mechanism which could describe the crystallization kinetics of neat polyesters and the blend.

The crystallization kinetics of PTT, PBT, and the blend possibly follows the AE2 (Nucleation growth) mechanism. AE2 mechanism in this case is a complex one and might be dominated by the properties and behavior of the growing crystal and the surrounding matrix.

This study has also demonstrated that the blend was inherently immiscible in the initially blended state and was confirmed by DSC studies. Annealing at high temperature (265 °C) for long-period of time (>9 min), the possible *trans*-reactions could occur between PTT, PBT, and PC.

Acknowledgments The author is grateful to the research department of Kuwait University for providing funds from project EC01/08 for carrying out this research study. He is grateful to Dr. Johnson Mathew and Divya Mary for the valuable help provided during the course of this study. He is also grateful to the analytical laboratory of chemistry department, Kuwait University for carrying out the ^{1}H NMR and FT-IR analysis. The authors are grateful to the research department of Kuwait University for providing funds for the General Facility GE 03/08 (nanotechnology lab) for carrying out this research.

References

1. Paul DR, Newman S (1978) Polymer blends, vols I and II. Academic, London
2. Utracki LA (1989) Polymer blends and alloys: thermodynamics and rheology. Hanser Publisher, Munich
3. Grebowicz J, Chauh HH (1996) Progress report. Shell Chemical Co., Houston, TX
4. Dangayach K, Chauh HH, Gergen W, Dalton P, Smith F (1997) Plastic-saving planet earth. Proceedings of 55th ANTEC conference, Toronto
5. Liau WB, Liu AS, Chiu WY (1999) Miscibility behaviors in poly(butylene terephthalate)/polyarylates based on bisphenol A copolymer blends. J Polym Res 6:27–33
6. Chiu FG, Huang KH, Yang JC (2003) Miscibility and thermal properties of melt-mixed poly(trimethylene terephthalate)/amorphous copolyester blends. J Polym Sci Phys: Part B, Polym Phys 41:2264–2274
7. Ramiro J, Eguiazabal JI, Nazabal J (2003) Synergistic mechanical behavior and improved processability of poly (ether imide) by blending with poly(trimethylene terephthalate). Polym Adv Technol 14:129–136
8. Supaphol P, Dangseeyum N, Thanomkiat P, Nithitanakul M (2004) Thermal, crystallization, mechanical, and rheological characteristics of poly(trimethylene terephthalate)/poly(ethylene terephthalate) blends. J Polym Sci: Part B Polym Phys 42:676–686
9. Yavari A, Asadinezhad A, Jafari SH, Khonakdar HA, Boehme F, Haessler R (2005) Effect of transesterification products on the miscibility and phase behavior of poly(trimethylene terephthalate)/bisphenol A polycarbonate blends. Eur Polym J 41:2880–2886
10. Xue ML, Sheng J, Chuah HH, Zhang XY (2004) Miscibility, morphology, and crystallization behavior of PTT/PC blends. J Macromol Sci Phys B 43:1045–1061
11. Xue ML, Yu YL, Sheng J, Chuah HH, Geng CH (2005) Compatibilization of poly(trimethylene terephthalate)/polycarbonate blends by epoxy. Part 1. Miscibility and morphology. J Macromol Sci Phys B 44:317–329
12. Chiu FC, Ting MH (2007) Thermal properties and phase morphology of melt-mixed poly(trimethylene terephthalate)/polycarbonate blends-mixing time effect. Polym Test 26:338–350
13. Lee LT, Woo EM (2003) Reaction-induced miscibility in blends comprised of bisphenol-A polycarbonate and poly(trimethylene terephthalate). Colloid Polym Sci 282:1308–1315

14. Na SK, Kong BG, Choi CY, Jang MK, Nah JW, Kim HG, Jo BW (2005) Transesterification and compatibilization in the blends of bisphenol-A polycarbonate and poly(trimethylene terephthalate). Macromol Res 13:88–95
15. Oh SJ, Chae DW, Lee HJ, Kim BC (2001) Study on polytrimethylene terephthalate-polycarbonate blends: effects of blending time and compositions on physical properties. Polym Mat Sci Eng 84:621–622
16. Xue ML, Yu YL, Sheng J, Chuah HH (2005) Crystallization behavior of poly(trimethylene terephthalate)/polycarbonate blends. J Macromol Sci Phys B 44:531–547
17. Bae WJ, Jo WH, Lee MS (2001) Solid state structure and mechanical properties of melt mixed poly(trimethylene terephthalate)/polycarbonate blends. Polym Mat Sci Eng 84:668–675
18. Bae WJ, Jo WH, Park YH (2002) Crystallization-induced sequential reordering in poly(trimethylene terephthalate)/polycarbonate blends. Macromol Res 10:145–149
19. Brown WE, Dollimore D, Galwey AK (1980) Reactions in the solid state. In: Bamford CH, Tipper CFH (eds) Comprehensive chemical kinetics, vol 22. Elsevier, Amsterdam
20. Wendlandt WW (1974) Thermal methods of analysis. Wiley, New York
21. Manche EP, Caroll B (1972) In: Caroll B (ed) Physical methods in macromolecular chemistry. Marcell-Dekker, New York
22. Kissinger HE (1956) Variation of peak temperature with heating rate in differential thermal analysis. J Res Nat Bur Stand 57:217–221
23. Matusita K, Sakka S, Matsui Y (1975) Determination of the activation energy for crystal growth by differential thermal analysis. J Mater Sci 10:961–966
24. Matusita K, Sakka S (1979) Kinetic study of the crystallization of glass by differential scanning calorimetry. Phys Chem Glasses 20:81–84
25. Matusita K, Sakka S (1980) Kinetic study of crystallization of glass by differential thermal analysis-criterion on application of Kissinger plots. J Non-Cryst Solids 38–39:741–774
26. Xu XJ, Ray CS, Day DE (1991) Nucleation and crystallization of $Na_2O\cdots 2CaO\cdots 3SiO_2$ glass by differential thermal analysis. J Am Ceram Soc 74:909–914
27. Kissinger HE (1957) Reactive kinetics in differential thermal analysis. Anal Chem Glasses 29:1702–1706
28. Mahadevan S, Giridhar A, Singh AK (1986) Calorimetric measurements on As–Sb–Se glasses. J Non-Cryst Solids 88:11–34
29. Matusita K, Komatsu T, Yokota R (1984) Kinetics of non-isothermal crystallization process and activation energy for crystal growth in amorphous materials. J Mater Sci 19:291–296
30. Colmenero J, Barandiaran JM (1978) Crystallization of $Al_{23}Te_{77}$ glasses. J Non-Cryst Solids 30:263–271
31. Afify N (1992) Calorimetric study on the crystallization of a $Se_{0.8}Te_{0.2}$ chalcogenide glass. J Non-Cryst Solids 142:247–259
32. Gao Z, Nakada M, Amasaki I (2001) A consideration of errors and accuracy in the isoconversional methods. Thermochim Acta 369:137–142
33. Avrami M (1939) Kinetics of phase change. I General theory. J Chem Phys 7:1103–1112
34. Avrami M (1940) Kinetics of phase change. II Transformation-time relations for random distribution of nuclei. J Chem Phys 8:212–225
35. Devaux J, Godard P, Mercier JP (1982) Bisphenol-A polycarbonate–poly(butylene terephthalate) transesterification. I. Theoretical study of the structure and of the degree of randomness in four-component copolycondensates. J Polym Sci, Part B: Polym Phys 20:1875–1880